

Measurement of Λ transverse polarization in e^+e^- collisions at $\sqrt{s} = 3.68 - 3.71$ GeV

The BESIII Collaboration



M. Ablikim¹, M. N. Achasov^{13,b}, P. Adlarson⁷³, R. Aliberti³⁴, A. Amoroso^{72A,72C},
M. R. An³⁸, Q. An^{69,56}, Y. Bai⁵⁵, O. Bakina³⁵, R. Baldini Ferroli^{28A}, I. Balossino^{29A},
Y. Ban^{45,g}, V. Batozskaya^{1,43}, D. Becker³⁴, K. Begzsuren³¹, N. Berger³⁴,
M. Bertani^{28A}, D. Bettoni^{29A}, F. Bianchi^{72A,72C}, E. Bianco^{72A,72C}, J. Bloms⁶⁶,
A. Bortone^{72A,72C}, I. Boyko³⁵, R. A. Briere⁵, A. Brueggemann⁶⁶, H. Cai⁷⁴, X. Cai^{1,56},
A. Calcaterra^{28A}, G. F. Cao^{1,61}, N. Cao^{1,61}, S. A. Cetin^{60A}, X. Y. Chai^{45,g},
J. F. Chang^{1,56}, T. T. Chang⁷⁵, W. L. Chang^{1,61}, G. R. Che⁴², G. Chelkov^{35,a},
C. Chen⁴², Chao Chen⁵³, G. Chen¹, H. S. Chen^{1,61}, M. L. Chen^{1,56,61}, S. J. Chen⁴¹,
S. M. Chen⁵⁹, T. Chen^{1,61}, X. R. Chen^{30,61}, X. T. Chen^{1,61}, Y. B. Chen^{1,56},
Y. Q. Chen³³, Z. J. Chen^{25,h}, W. S. Cheng^{72C}, S. K. Choi¹⁰, X. Chu⁴²,
G. Cibinetto^{29A}, S. C. Coen⁴, F. Cossio^{72C}, J. J. Cui⁴⁸, H. L. Dai^{1,56}, J. P. Dai⁷⁷,
A. Dbeyssi¹⁹, R. E. de Boer⁴, D. Dedovich³⁵, Z. Y. Deng¹, A. Denig³⁴,
I. Denysenko³⁵, M. Destefanis^{72A,72C}, F. De Mori^{72A,72C}, Y. Ding³⁹, Y. Ding³³,
J. Dong^{1,56}, L. Y. Dong^{1,61}, M. Y. Dong^{1,56,61}, X. Dong⁷⁴, S. X. Du⁷⁹, Z. H. Duan⁴¹,
P. Egorov^{35,a}, Y. L. Fan⁷⁴, J. Fang^{1,56}, S. S. Fang^{1,61}, W. X. Fang¹, Y. Fang¹,
R. Farinelli^{29A}, L. Fava^{72B,72C}, F. Feldbauer⁴, G. Felici^{28A}, C. Q. Feng^{69,56},
J. H. Feng⁵⁷, K. Fischer⁶⁷, M. Fritsch⁴, C. Fritsch⁶⁶, C. D. Fu¹, Y. W. Fu¹, H. Gao⁶¹,
Y. N. Gao^{45,g}, Yang Gao^{69,56}, S. Garbolino^{72C}, I. Garzia^{29A,29B}, P. T. Ge⁷⁴,
Z. W. Ge⁴¹, C. Geng⁵⁷, E. M. Gersabeck⁶⁵, A. Gilman⁶⁷, K. Goetzen¹⁴, L. Gong³⁹,
W. X. Gong^{1,56}, W. Gradl³⁴, M. Greco^{72A,72C}, M. H. Gu^{1,56}, Y. T. Gu¹⁶,
C. Y. Guan^{1,61}, Z. L. Guan²², A. Q. Guo^{30,61}, L. B. Guo⁴⁰, R. P. Guo⁴⁷, Y. P. Guo^{12,f},
A. Guskov^{35,a}, X. T. H.^{1,61}, W. Y. Han³⁸, X. Q. Hao²⁰, F. A. Harris⁶³, K. K. He⁵³,
K. L. He^{1,61}, F. H. Heinsius⁴, C. H. Heinz³⁴, Y. K. Heng^{1,56,61}, C. Herold⁵⁸,
T. Holtmann⁴, P. C. Hong^{12,f}, G. Y. Hou^{1,61}, Y. R. Hou⁶¹, Z. L. Hou¹, H. M. Hu^{1,61},
J. F. Hu^{54,i}, T. Hu^{1,56,61}, Y. Hu¹, G. S. Huang^{69,56}, K. X. Huang⁵⁷, L. Q. Huang^{30,61},
X. T. Huang⁴⁸, Y. P. Huang¹, T. Hussain⁷¹, N. Hüsken^{27,34}, W. Imoehl²⁷,
M. Irshad^{69,56}, J. Jackson²⁷, S. Jaeger⁴, S. Janchiv³¹, J. H. Jeong¹⁰, Q. Ji¹,
Q. P. Ji²⁰, X. B. Ji^{1,61}, X. L. Ji^{1,56}, Y. Y. Ji⁴⁸, Z. K. Jia^{69,56}, P. C. Jiang^{45,g},
S. S. Jiang³⁸, T. J. Jiang¹⁷, X. S. Jiang^{1,56,61}, Y. Jiang⁶¹, J. B. Jiao⁴⁸, Z. Jiao²³,
S. Jin⁴¹, Y. Jin⁶⁴, M. Q. Jing^{1,61}, T. Johansson⁷³, X. K.¹, S. K. Kabana³²,

N. Kalantar-Nayestanaki⁶², X. L. Kang⁹, X. S. Kang³⁹, R. Kappert⁶²,
M. Kavatsyuk⁶², B. C. Ke⁷⁹, A. Khoukaz⁶⁶, R. Kiuchi¹, R. Kliemt¹⁴, L. Koch³⁶,
O. B. Kolcu^{60A}, B. Kopf⁴, M. Kuessner⁴, A. Kupsc^{43,73}, W. Kühn³⁶, J. J. Lane⁶⁵,
J. S. Lange³⁶, P. Larin¹⁹, A. Lavania²⁶, L. Lavezzi^{72A,72C}, T. T. Lei^{69,k}, Z. H. Lei^{69,56},
H. Leithoff³⁴, M. Lellmann³⁴, T. Lenz³⁴, C. Li⁴², C. Li⁴⁶, C. H. Li³⁸, Cheng Li^{69,56},
D. M. Li⁷⁹, F. Li^{1,56}, G. Li¹, H. Li^{69,56}, H. B. Li^{1,61}, H. J. Li²⁰, H. N. Li^{54,i}, Hui Li⁴²,
J. R. Li⁵⁹, J. S. Li⁵⁷, J. W. Li⁴⁸, Ke Li¹, L. J. Li^{1,61}, L. K. Li¹, Lei Li³, M. H. Li⁴²,
P. R. Li^{37,j,k}, S. X. Li¹², S. Y. Li⁵⁹, T. Li⁴⁸, W. D. Li^{1,61}, W. G. Li¹, X. H. Li^{69,56},
X. L. Li⁴⁸, Xiaoyu Li^{1,61}, Y. G. Li^{45,g}, Z. J. Li⁵⁷, Z. X. Li¹⁶, Z. Y. Li⁵⁷, C. Liang⁴¹,
H. Liang^{1,61}, H. Liang³³, H. Liang^{69,56}, Y. F. Liang⁵², Y. T. Liang^{30,61}, G. R. Liao¹⁵,
L. Z. Liao⁴⁸, J. Libby²⁶, A. Limphirat⁵⁸, D. X. Lin^{30,61}, T. Lin¹, B. X. Liu⁷⁴,
B. J. Liu¹, C. Liu³³, C. X. Liu¹, D. Liu^{19,69}, F. H. Liu⁵¹, Fang Liu¹, Feng Liu⁶,
G. M. Liu^{54,i}, H. Liu^{37,j,k}, H. B. Liu¹⁶, H. M. Liu^{1,61}, Huanhuan Liu¹, Huihui Liu²¹,
J. B. Liu^{69,56}, J. L. Liu⁷⁰, J. Y. Liu^{1,61}, K. Liu¹, K. Y. Liu³⁹, Ke Liu²², L. Liu^{69,56},
L. C. Liu⁴², Lu Liu⁴², M. H. Liu^{12,f}, P. L. Liu¹, Q. Liu⁶¹, S. B. Liu^{69,56}, T. Liu^{12,f},
W. K. Liu⁴², W. M. Liu^{69,56}, X. Liu^{37,j,k}, Y. Liu^{37,j,k}, Y. B. Liu⁴², Z. A. Liu^{1,56,61},
Z. Q. Liu⁴⁸, X. C. Lou^{1,56,61}, F. X. Lu⁵⁷, H. J. Lu²³, J. G. Lu^{1,56}, X. L. Lu¹, Y. Lu⁷,
Y. P. Lu^{1,56}, Z. H. Lu^{1,61}, C. L. Luo⁴⁰, M. X. Luo⁷⁸, T. Luo^{12,f}, X. L. Luo^{1,56},
X. R. Lyu⁶¹, Y. F. Lyu⁴², F. C. Ma³⁹, H. L. Ma¹, J. L. Ma^{1,61}, L. L. Ma⁴⁸,
M. M. Ma^{1,61}, Q. M. Ma¹, R. Q. Ma^{1,61}, R. T. Ma⁶¹, X. Y. Ma^{1,56}, Y. Ma^{45,g},
F. E. Maas¹⁹, M. Maggiora^{72A,72C}, S. Maldaner⁴, S. Malde⁶⁷, A. Mangoni^{28B},
Y. J. Mao^{45,g}, Z. P. Mao¹, S. Marcello^{72A,72C}, Z. X. Meng⁶⁴, J. G. Messchendorp^{14,62},
G. Mezzadri^{29A}, H. Miao^{1,61}, T. J. Min⁴¹, R. E. Mitchell²⁷, X. H. Mo^{1,56,61},
N. Yu. Muchnoi^{13,b}, Y. Nefedov³⁵, F. Nerling^{19,d}, I. B. Nikolaev^{13,b}, Z. Ning^{1,56},
S. Nisar^{11,l}, Y. Niu⁴⁸, S. L. Olsen⁶¹, Q. Ouyang^{1,56,61}, S. Pacetti^{28B,28C}, X. Pan⁵³,
Y. Pan⁵⁵, A. Pathak³³, Y. P. Pei^{69,56}, M. Pelizaeus⁴, H. P. Peng^{69,56}, K. Peters^{14,d},
J. L. Ping⁴⁰, R. G. Ping^{1,61}, S. Plura³⁴, S. Pogodin³⁵, V. Prasad^{69,56}, V. P. Prasad³²,
F. Z. Qi¹, H. Qi^{69,56}, H. R. Qi⁵⁹, M. Qi⁴¹, T. Y. Qi^{12,f}, S. Qian^{1,56}, W. B. Qian⁶¹,
C. F. Qiao⁶¹, J. J. Qin⁷⁰, L. Q. Qin¹⁵, X. P. Qin^{12,f}, X. S. Qin⁴⁸, Z. H. Qin^{1,56},
J. F. Qiu¹, S. Q. Qu⁵⁹, C. F. Redmer³⁴, K. J. Ren³⁸, A. Rivetti^{72C}, V. Rodin⁶²,
M. Rolo^{72C}, G. Rong^{1,61}, Ch. Rosner¹⁹, S. N. Ruan⁴², A. Sarantsev^{35,c},
Y. Schelhaas³⁴, K. Schoenning⁷³, M. Scodeggio^{29A,29B}, K. Y. Shan^{12,f}, W. Shan²⁴,
X. Y. Shan^{69,56}, J. F. Shangguan⁵³, L. G. Shao^{1,61}, M. Shao^{69,56}, C. P. Shen^{12,f},
H. F. Shen^{1,61}, W. H. Shen⁶¹, X. Y. Shen^{1,61}, B. A. Shi⁶¹, H. C. Shi^{69,56}, J. Y. Shi¹,
Q. Q. Shi⁵³, R. S. Shi^{1,61}, X. Shi^{1,56}, J. J. Song²⁰, T. Z. Song⁵⁷, W. M. Song^{33,1},
Y. X. Song^{45,g}, S. Sosio^{72A,72C}, S. Spataro^{72A,72C}, F. Stieler³⁴, Y. J. Su⁶¹,
G. B. Sun⁷⁴, G. X. Sun¹, H. Sun⁶¹, H. K. Sun¹, J. F. Sun²⁰, K. Sun⁵⁹, L. Sun⁷⁴,
S. S. Sun^{1,61}, T. Sun^{1,61}, W. Y. Sun³³, Y. Sun⁹, Y. J. Sun^{69,56}, Y. Z. Sun¹,
Z. T. Sun⁴⁸, Y. X. Tan^{69,56}, C. J. Tang⁵², G. Y. Tang¹, J. Tang⁵⁷, Y. A. Tang⁷⁴,
L. Y. Tao⁷⁰, Q. T. Tao^{25,h}, M. Tat⁶⁷, J. X. Teng^{69,56}, V. Thoren⁷³, W. H. Tian⁵⁰,
W. H. Tian⁵⁷, Y. Tian^{30,61}, Z. F. Tian⁷⁴, I. Uman^{60B}, B. Wang¹, B. Wang^{69,56},
B. L. Wang⁶¹, C. W. Wang⁴¹, D. Y. Wang^{45,g}, F. Wang⁷⁰, H. J. Wang^{37,j,k},
H. P. Wang^{1,61}, K. Wang^{1,56}, L. L. Wang¹, M. Wang⁴⁸, Meng Wang^{1,61}, S. Wang^{12,f},

T. Wang^{12,f}, T. J. Wang⁴², W. Wang⁷⁰, W. Wang⁵⁷, W. H. Wang⁷⁴,
W. P. Wang^{69,56}, X. Wang^{45,g}, X. F. Wang^{37,j,k}, X. J. Wang³⁸, X. L. Wang^{12,f},
Y. Wang⁵⁹, Y. D. Wang⁴⁴, Y. F. Wang^{1,56,61}, Y. H. Wang⁴⁶, Y. N. Wang⁴⁴,
Y. Q. Wang¹, Yaqian Wang^{18,1}, Yi Wang⁵⁹, Z. Wang^{1,56}, Z. L. Wang⁷⁰,
Z. Y. Wang^{1,61}, Ziyi Wang⁶¹, D. Wei⁶⁸, D. H. Wei¹⁵, F. Weidner⁶⁶, S. P. Wen¹,
C. W. Wenzel⁴, U. Wiedner⁴, G. Wilkinson⁶⁷, M. Wolke⁷³, L. Wollenberg⁴, C. Wu³⁸,
J. F. Wu^{1,61}, L. H. Wu¹, L. J. Wu^{1,61}, X. Wu^{12,f}, X. H. Wu³³, Y. Wu⁶⁹, Y. J. Wu³⁰,
Z. Wu^{1,56}, L. Xia^{69,56}, X. M. Xian³⁸, T. Xiang^{45,g}, D. Xiao^{37,j,k}, G. Y. Xiao⁴¹,
H. Xiao^{12,f}, S. Y. Xiao¹, Y. L. Xiao^{12,f}, Z. J. Xiao⁴⁰, C. Xie⁴¹, X. H. Xie^{45,g},
Y. Xie⁴⁸, Y. G. Xie^{1,56}, Y. H. Xie⁶, Z. P. Xie^{69,56}, T. Y. Xing^{1,61}, C. F. Xu^{1,61},
C. J. Xu⁵⁷, G. F. Xu¹, H. Y. Xu⁶⁴, Q. J. Xu¹⁷, X. P. Xu⁵³, Y. C. Xu⁷⁶, Z. P. Xu⁴¹,
F. Yan^{12,f}, L. Yan^{12,f}, W. B. Yan^{69,56}, W. C. Yan⁷⁹, X. Q. Yan¹, H. J. Yang^{49,e},
H. L. Yang³³, H. X. Yang¹, Tao Yang¹, Y. Yang^{12,f}, Y. F. Yang⁴², Y. X. Yang^{1,61},
Yifan Yang^{1,61}, M. Ye^{1,56}, M. H. Ye⁸, J. H. Yin¹, Z. Y. You⁵⁷, B. X. Yu^{1,56,61},
C. X. Yu⁴², G. Yu^{1,61}, T. Yu⁷⁰, X. D. Yu^{45,g}, C. Z. Yuan^{1,61}, L. Yuan², S. C. Yuan¹,
X. Q. Yuan¹, Y. Yuan^{1,61}, Z. Y. Yuan⁵⁷, C. X. Yue³⁸, A. A. Zafar⁷¹, F. R. Zeng⁴⁸,
X. Zeng^{12,f}, Y. Zeng^{25,h}, X. Y. Zhai³³, Y. H. Zhan⁵⁷, A. Q. Zhang^{1,61},
B. L. Zhang^{1,61}, B. X. Zhang¹, D. H. Zhang⁴², G. Y. Zhang²⁰, H. Zhang⁶⁹,
H. H. Zhang⁵⁷, H. H. Zhang³³, H. Q. Zhang^{1,56,61}, H. Y. Zhang^{1,56}, J. J. Zhang⁵⁰,
J. L. Zhang⁷⁵, J. Q. Zhang⁴⁰, J. W. Zhang^{1,56,61}, J. X. Zhang^{37,j,k}, J. Y. Zhang¹,
J. Z. Zhang^{1,61}, Jianyu Zhang^{1,61}, Jiawei Zhang^{1,61}, L. M. Zhang⁵⁹, L. Q. Zhang⁵⁷,
Lei Zhang⁴¹, P. Zhang¹, Q. Y. Zhang^{38,79}, Shuihan Zhang^{1,61}, Shulei Zhang^{25,h},
X. D. Zhang⁴⁴, X. M. Zhang¹, X. Y. Zhang⁵³, X. Y. Zhang⁴⁸, Y. Zhang⁶⁷, Y.
T. Zhang⁷⁹, Y. H. Zhang^{1,56}, Yan Zhang^{69,56}, Yao Zhang¹, Z. H. Zhang¹,
Z. L. Zhang³³, Z. Y. Zhang⁴², Z. Y. Zhang⁷⁴, G. Zhao¹, J. Zhao³⁸, J. Y. Zhao^{1,61},
J. Z. Zhao^{1,56}, Lei Zhao^{69,56}, Ling Zhao¹, M. G. Zhao⁴², S. J. Zhao⁷⁹, Y. B. Zhao^{1,56},
Y. X. Zhao^{30,61}, Z. G. Zhao^{69,56}, A. Zhemchugov^{35,a}, B. Zheng⁷⁰, J. P. Zheng^{1,56},
W. J. Zheng^{1,61}, Y. H. Zheng⁶¹, B. Zhong⁴⁰, X. Zhong⁵⁷, H. Zhou⁴⁸, L. P. Zhou^{1,61},
X. Zhou⁷⁴, X. K. Zhou⁶¹, X. R. Zhou^{69,56}, X. Y. Zhou³⁸, Y. Z. Zhou^{12,f}, J. Zhu⁴²,
K. Zhu¹, K. J. Zhu^{1,56,61}, L. Zhu³³, L. X. Zhu⁶¹, S. H. Zhu⁶⁸, S. Q. Zhu⁴¹,
T. J. Zhu^{12,f}, W. J. Zhu^{12,f}, Y. C. Zhu^{69,56}, Z. A. Zhu^{1,61}, J. H. Zou¹, J. Zu^{69,56}

(BESIII Collaboration)

¹ *Institute of High Energy Physics, Beijing 100049, People's Republic of China*

² *Beihang University, Beijing 100191, People's Republic of China*

³ *Beijing Institute of Petrochemical Technology, Beijing 102617, People's Republic of China*

⁴ *Bochum Ruhr-University, D-44780 Bochum, Germany*

⁵ *Carnegie Mellon University, Pittsburgh, Pennsylvania 15213, USA*

⁶ *Central China Normal University, Wuhan 430079, People's Republic of China*

⁷ *Central South University, Changsha 410083, People's Republic of China*

⁸ *China Center of Advanced Science and Technology, Beijing 100190, People's Republic of China*

- ⁹ *China University of Geosciences, Wuhan 430074, People's Republic of China*
- ¹⁰ *Chung-Ang University,*
- ¹¹ *COMSATS University Islamabad, Lahore Campus, Defence Road, Off Raiwind Road, 54000 Lahore, Pakistan*
- ¹² *Fudan University, Shanghai 200433, People's Republic of China*
- ¹³ *G.I. Budker Institute of Nuclear Physics SB RAS (BINP), Novosibirsk 630090, Russia*
- ¹⁴ *GSI Helmholtzcentre for Heavy Ion Research GmbH, D-64291 Darmstadt, Germany*
- ¹⁵ *Guangxi Normal University, Guilin 541004, People's Republic of China*
- ¹⁶ *Guangxi University, Nanning 530004, People's Republic of China*
- ¹⁷ *Hangzhou Normal University, Hangzhou 310036, People's Republic of China*
- ¹⁸ *Hebei University, Baoding 071002, People's Republic of China*
- ¹⁹ *Helmholtz Institute Mainz, Staudinger Weg 18, D-55099 Mainz, Germany*
- ²⁰ *Henan Normal University, Xinxiang 453007, People's Republic of China*
- ²¹ *Henan University of Science and Technology, Luoyang 471003, People's Republic of China*
- ²² *Henan University of Technology, Zhengzhou 450001, People's Republic of China*
- ²³ *Huangshan College, Huangshan 245000, People's Republic of China*
- ²⁴ *Hunan Normal University, Changsha 410081, People's Republic of China*
- ²⁵ *Hunan University, Changsha 410082, People's Republic of China*
- ²⁶ *Indian Institute of Technology Madras, Chennai 600036, India*
- ²⁷ *Indiana University, Bloomington, Indiana 47405, USA*
- ²⁸ *INFN Laboratori Nazionali di Frascati , (A)INFN Laboratori Nazionali di Frascati, I-00044, Frascati, Italy; (B)INFN Sezione di Perugia, I-06100, Perugia, Italy; (C)University of Perugia, I-06100, Perugia, Italy*
- ²⁹ *INFN Sezione di Ferrara, (A)INFN Sezione di Ferrara, I-44122, Ferrara, Italy; (B)University of Ferrara, I-44122, Ferrara, Italy*
- ³⁰ *Institute of Modern Physics, Lanzhou 730000, People's Republic of China*
- ³¹ *Institute of Physics and Technology, Peace Avenue 54B, Ulaanbaatar 13330, Mongolia*
- ³² *Instituto de Alta Investigación, Universidad de Tarapacá, Casilla 7D, Arica, Chile*
- ³³ *Jilin University, Changchun 130012, People's Republic of China*
- ³⁴ *Johannes Gutenberg University of Mainz, Johann-Joachim-Becher-Weg 45, D-55099 Mainz, Germany*
- ³⁵ *Joint Institute for Nuclear Research, 141980 Dubna, Moscow region, Russia*
- ³⁶ *Justus-Liebig-Universitaet Giessen, II. Physikalisches Institut, Heinrich-Buff-Ring 16, D-35392 Giessen, Germany*
- ³⁷ *Lanzhou University, Lanzhou 730000, People's Republic of China*
- ³⁸ *Liaoning Normal University, Dalian 116029, People's Republic of China*
- ³⁹ *Liaoning University, Shenyang 110036, People's Republic of China*
- ⁴⁰ *Nanjing Normal University, Nanjing 210023, People's Republic of China*
- ⁴¹ *Nanjing University, Nanjing 210093, People's Republic of China*
- ⁴² *Nankai University, Tianjin 300071, People's Republic of China*
- ⁴³ *National Centre for Nuclear Research, Warsaw 02-093, Poland*
- ⁴⁴ *North China Electric Power University, Beijing 102206, People's Republic of China*

- ⁴⁵ *Peking University, Beijing 100871, People's Republic of China*
- ⁴⁶ *Qufu Normal University, Qufu 273165, People's Republic of China*
- ⁴⁷ *Shandong Normal University, Jinan 250014, People's Republic of China*
- ⁴⁸ *Shandong University, Jinan 250100, People's Republic of China*
- ⁴⁹ *Shanghai Jiao Tong University, Shanghai 200240, People's Republic of China*
- ⁵⁰ *Shanxi Normal University, Linfen 041004, People's Republic of China*
- ⁵¹ *Shanxi University, Taiyuan 030006, People's Republic of China*
- ⁵² *Sichuan University, Chengdu 610064, People's Republic of China*
- ⁵³ *Soochow University, Suzhou 215006, People's Republic of China*
- ⁵⁴ *South China Normal University, Guangzhou 510006, People's Republic of China*
- ⁵⁵ *Southeast University, Nanjing 211100, People's Republic of China*
- ⁵⁶ *State Key Laboratory of Particle Detection and Electronics, Beijing 100049, Hefei 230026, People's Republic of China*
- ⁵⁷ *Sun Yat-Sen University, Guangzhou 510275, People's Republic of China*
- ⁵⁸ *Suranaree University of Technology, University Avenue 111, Nakhon Ratchasima 30000, Thailand*
- ⁵⁹ *Tsinghua University, Beijing 100084, People's Republic of China*
- ⁶⁰ *Turkish Accelerator Center Particle Factory Group, (A)Istinye University, 34010, Istanbul, Turkey; (B)Near East University, Nicosia, North Cyprus, 99138, Mersin 10, Turkey*
- ⁶¹ *University of Chinese Academy of Sciences, Beijing 100049, People's Republic of China*
- ⁶² *University of Groningen, NL-9747 AA Groningen, The Netherlands*
- ⁶³ *University of Hawaii, Honolulu, Hawaii 96822, USA*
- ⁶⁴ *University of Jinan, Jinan 250022, People's Republic of China*
- ⁶⁵ *University of Manchester, Oxford Road, Manchester, M13 9PL, United Kingdom*
- ⁶⁶ *University of Muenster, Wilhelm-Klemm-Strasse 9, 48149 Muenster, Germany*
- ⁶⁷ *University of Oxford, Keble Road, Oxford OX13RH, United Kingdom*
- ⁶⁸ *University of Science and Technology Liaoning, Anshan 114051, People's Republic of China*
- ⁶⁹ *University of Science and Technology of China, Hefei 230026, People's Republic of China*
- ⁷⁰ *University of South China, Hengyang 421001, People's Republic of China*
- ⁷¹ *University of the Punjab, Lahore-54590, Pakistan*
- ⁷² *University of Turin and INFN, (A)University of Turin, I-10125, Turin, Italy; (B)University of Eastern Piedmont, I-15121, Alessandria, Italy; (C)INFN, I-10125, Turin, Italy*
- ⁷³ *Uppsala University, Box 516, SE-75120 Uppsala, Sweden*
- ⁷⁴ *Wuhan University, Wuhan 430072, People's Republic of China*
- ⁷⁵ *Xinyang Normal University, Xinyang 464000, People's Republic of China*
- ⁷⁶ *Yantai University, Yantai 264005, People's Republic of China*
- ⁷⁷ *Yunnan University, Kunming 650500, People's Republic of China*
- ⁷⁸ *Zhejiang University, Hangzhou 310027, People's Republic of China*
- ⁷⁹ *Zhengzhou University, Zhengzhou 450001, People's Republic of China*

- ^a Also at the Moscow Institute of Physics and Technology, Moscow 141700, Russia
- ^b Also at the Novosibirsk State University, Novosibirsk, 630090, Russia
- ^c Also at the NRC "Kurchatov Institute", PNPI, 188300, Gatchina, Russia
- ^d Also at Goethe University Frankfurt, 60323 Frankfurt am Main, Germany
- ^e Also at Key Laboratory for Particle Physics, Astrophysics and Cosmology, Ministry of Education; Shanghai Key Laboratory for Particle Physics and Cosmology; Institute of Nuclear and Particle Physics, Shanghai 200240, People's Republic of China
- ^f Also at Key Laboratory of Nuclear Physics and Ion-beam Application (MOE) and Institute of Modern Physics, Fudan University, Shanghai 200443, People's Republic of China
- ^g Also at State Key Laboratory of Nuclear Physics and Technology, Peking University, Beijing 100871, People's Republic of China
- ^h Also at School of Physics and Electronics, Hunan University, Changsha 410082, China
- ⁱ Also at Guangdong Provincial Key Laboratory of Nuclear Science, Institute of Quantum Matter, South China Normal University, Guangzhou 510006, China
- ^j Also at Frontiers Science Center for Rare Isotopes, Lanzhou University, Lanzhou 730000, People's Republic of China
- ^k Also at Lanzhou Center for Theoretical Physics, Key Laboratory of Theoretical Physics of Gansu Province, and Key Laboratory for Quantum Theory and Applications of MoE, Lanzhou University, Lanzhou 730000, People's Republic of China
- ^l Also at the Department of Mathematical Sciences, IBA, Karachi, Pakistan

E-mail: besiii-publications@ihep.ac.cn

ABSTRACT: With data samples collected with the BESIII detector at seven energy points at $\sqrt{s} = 3.68 - 3.71$ GeV, corresponding to an integrated luminosity of 333 pb^{-1} , we present a study of the Λ transverse polarization in the $e^+e^- \rightarrow \Lambda\bar{\Lambda}$ reaction. The significance of polarization by combining the seven energy points is found to be 2.6σ including the systematic uncertainty, which implies a non-zero phase between the transition amplitudes of the $\Lambda\bar{\Lambda}$ helicity states. The modulus ratio and the relative phase of EM-*psionic* form factors combined with all energy points are measured to be $R^\Psi = 0.71_{-0.10}^{+0.10} \pm 0.03$ and $\Delta\Phi^\Psi = 23_{-8.0}^{+8.8} \pm 1.6^\circ$, where the first uncertainties are statistical and the second systematic.

Contents

1	Introduction	1
2	BESIII detector and Monte Carlo simulation	2
3	Event selection	3
4	Extraction of Λ polarization	4
5	Systematic uncertainties	9
5.1	Λ reconstruction	9
5.2	Mass window	9
5.3	4C kinematic fit	9
5.4	Background	9
5.5	Fit method	9
5.6	Decay parameter	9
5.7	Summary of systematic uncertainty	9
6	Summary	10

1 Introduction

The understanding of the structure of baryons is a very important issue in contemporary physics [1–6]. In the context of the Quantum Chromodynamics (QCD), it is particularly interesting to measure the electromagnetic form factors (EMFFs) of nucleons and hyperons, which are expected to reveal the aspects of the QCD description of the hyperon structure. In the 1960s, Cabibbo *et al.* [7] first proposed that time-like EMFFs could be studied on e^+e^- experiments by measuring the baryon pair production cross sections. Among them, the proton is a stable particle, and can be available as a target to study its space-like EMFFs by means of scattering experiments. This case is different from the unstable hyperons with finite lifetime which cannot be used in such scattering experiments. The advantage is that their weak parity-violating decay gives straightforward access to the polarization. The time-like form factors are related to more intuitive quantities such as charge and magnetization densities by dispersion relations [8, 9]. The production of spin-1/2 baryon-anti-baryon pairs from e^+e^- collisions is described by two independent parameters, the electric form factor G_E and the magnetic form factor G_M [10, 11].

They are both analytic functions of the four-momentum transfer squared q^2 . In the time-like region, starting from the threshold, corresponding to the squared mass of the lightest hadronic state that can couple to the intermediate virtual photon, the EMFFs are

complex. In particular, the complex value of their ratio implies a polarization effect in the final state baryons even when the initial state leptons are unpolarized. This provides a handle to understand the intrinsic structure of hyperons better.

Up to now, experimental data on hyperon EMFFs are very limited. The first determination of Λ EMFFs was reported by the BABAR collaboration [12] using the initial state radiation (ISR) method for the $e^+e^- \rightarrow \Lambda\bar{\Lambda}$ process. It measured the effective form factor, which is proportional to the total cross section assuming one-photon exchange. The cross section and EMFFs of some baryon pairs (p , Λ , Σ^0 , Ξ^- , and Ω^-) were determined by the CLEO collaboration [13, 14]. Their conclusions regarding EMFFs and di-quark correlations [15, 16] rely on the assumption that one-photon exchange dominates the production process and that decaying charmonia contributions are negligible. The BESIII collaboration has also measured cross sections of some baryon pairs (Λ , Σ^0 , Ξ^- , Σ^\pm , Ξ^0 and Ω^-) near the production threshold [17–22] and above the open charm threshold [23–25], while the experimental investigations of the relative phase between G_E and G_M are still limited.

At the resonances of vector charmonia, the spin formalism [26] is valid. In these cases, the amplitudes no longer represent EMFFs but instead the so-called EM-*psionic* form factors, G_E^Ψ and G_M^Ψ [27]. And the polarization is determined by the relative difference of electric and magnetic form factors $\Delta\Phi^\Psi \equiv \Phi_E^\Psi - \Phi_M^\Psi$, with $G_{E,M} = |G_{E,M}| e^{i\Phi_{E,M}}$, which were neglected in previous studies [19, 20, 23, 28–34]. Recently the Λ polarization was observed and measured in the $e^+e^- \rightarrow \Lambda\bar{\Lambda}$ process by the BESIII collaboration in J/ψ , $\psi(3770)$ and off-resonance regions [27, 35–37]. Subsequently, the Σ^+ hyperon polarization was observed by the BESIII collaboration in $e^+e^- \rightarrow J/\psi, \psi(3686) \rightarrow \Sigma^+\bar{\Sigma}^-$ processes [38]. The results reveal not only a non-zero relative psionic phase, but also that the phase changes sign at the $\psi(3686)$ mass with respect to the value measured at the J/ψ resonance. In the $e^+e^- \rightarrow J/\psi, \psi(3686) \rightarrow \Xi^-\bar{\Xi}^+$ channel [39–41], a non-zero polarization has also been observed for the Ξ^- hyperon. The energy points around 3.686 GeV are interesting in this regard since the production occurs through an interplay of one-photon exchange [37], mixing with $\psi(3770)$ resonance [27] and resonance dominating only [35, 36]. The large data samples corresponding to an integrated luminosity of 333 pb^{-1} , collected at $\sqrt{s} = 3.680, 3.683, 3.684, 3.685, 3.687, 3.691, \text{ and } 3.710 \text{ GeV}$ with the BESIII detector [42] recording symmetric e^+e^- collisions provided by the BEPCII storage ring [43], enable the study of this phenomenon, which we present in this article.

2 BESIII detector and Monte Carlo simulation

The BESIII detector [42] records symmetric e^+e^- collisions provided by the BEPCII storage ring [43] in the center-of-mass (CM) energy range from 2.0 to 4.95 GeV, with a peak luminosity of $1 \times 10^{33} \text{ cm}^{-2}\text{s}^{-1}$ achieved at $\sqrt{s} = 3.77 \text{ GeV}$. BESIII has collected large data samples in this energy region [44]. The cylindrical core of the BESIII detector covers 93% of the full solid angle and consists of a helium-based multilayer drift chamber (MDC), a plastic scintillator time-of-flight system (TOF), and a CsI(Tl) electromagnetic calorimeter (EMC), which are all enclosed in a superconducting solenoidal magnet providing a 1.0 T magnetic field. The magnetic field was 0.9 T in 2012, which affects 100% of the total J/ψ data. The

solenoid is supported by an octagonal flux-return yoke with resistive plate counter muon identification modules interleaved with steel. The charged-particle momentum resolution at 1 GeV/ c is 0.5%, and the dE/dx resolution is 6% for electrons from Bhabha scattering. The EMC measures photon energies with a resolution of 2.5% (5%) at 1 GeV in the barrel (end cap) region. The time resolution in the TOF barrel region is 68 ps, while that in the end cap region is 110 ps. The end cap TOF system was upgraded in 2015 using multigap resistive plate chamber technology, providing a time resolution of 60 ps, which benefits 100% of the data used in this analysis [45–47].

Simulated data samples produced with a GEANT4-based [48] Monte Carlo (MC) package, which includes the geometric description of the BESIII detector [49] and the detector response, are used to determine detection efficiencies and to estimate backgrounds. The simulation models the beam energy spread and ISR in the e^+e^- annihilation using the generator KKMC [50]. The detection efficiency for $e^+e^- \rightarrow \Lambda\bar{\Lambda}$ is determined by MC simulations. A sample of 1,000,000 events is simulated with a uniform phase space (PHSP) distribution for each of 7 CM energy points from 3.68 GeV to 3.71 GeV. The Λ baryon and its subsequent decays are handled by the EVTGEN program [51, 52] with PHSP model. The production process is simulated by the KKMC generator that includes the beam energy spread and ISR [53] in the e^+e^- annihilation.

3 Event selection

The full reconstruction method is performed to proceed event selection with the decay processes $\Lambda \rightarrow p\pi^-$ and $\bar{\Lambda} \rightarrow \bar{p}\pi^+$. There are four charged particles in the final state, a proton, an anti-proton and two charged pions from $\Lambda\bar{\Lambda}$. Thus, good candidates should satisfy the event selection criteria below.

Charged tracks are required to be reconstructed in the MDC within its angular coverage: $|\cos\theta| < 0.93$, where θ is defined with respect to the z axis, which is the symmetry axis of the MDC in the laboratory system. Events with at least two negative-charged tracks and two positive-charged tracks are kept for further analysis. Tracks with momentum larger than 0.6 GeV/ c are considered as proton candidates, and others are assumed to be pion candidates. Events with at least one proton, one anti-proton, one π^+ , and one π^- are retained for further analysis.

To reconstruct $\Lambda(\bar{\Lambda})$ candidates, a secondary vertex fit [54] is applied to all combinations of $p\pi^-(\bar{p}\pi^+)$ within one event. The pair of Λ and $\bar{\Lambda}$ candidates with the minimum value of $\sqrt{(M_{p\pi^-} - m_\Lambda)^2 + (M_{\bar{p}\pi^+} - m_\Lambda)^2}$ is selected. Here, $M_{p\pi^-(\bar{p}\pi^+)}$ is the invariant mass of the $p\pi^-(\bar{p}\pi^+)$ pair. To further suppress background from non- Λ events, the decay length of Λ candidate, i.e., the distance between its production and decay positions, is required to be greater than zero.

To further suppress background contributions and improve the mass resolution, a four-constraint (4C) kinematic fit imposing energy-momentum conservation from the initial e^+e^- to the final $\Lambda\bar{\Lambda}$ state is applied for all $\Lambda\bar{\Lambda}$ hypotheses after the $\Lambda(\bar{\Lambda})$ reconstruction, with the requirement of $\chi_{4C}^2 < 200$. Figure 1 shows the distribution of $M_{\bar{p}\pi^+}$ versus $M_{p\pi^-}$ after performing the 4C kinematic fit. A clear accumulation of events around m_Λ can be seen.

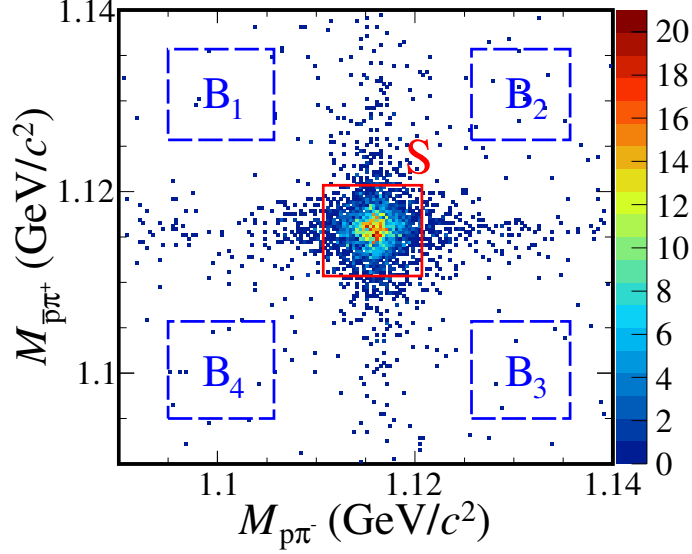


Figure 1. Two-dimensional distribution of $M_{p\bar{\pi}^+}$ versus $M_{p\pi^-}$ for all data samples, where the red solid box indicates the signal region, the blue dash boxes show the selected background regions.

4 Extraction of Λ polarization

The exclusive process $e^+e^- \rightarrow \gamma^*/\Psi \rightarrow \Lambda\bar{\Lambda} \rightarrow p\bar{p}\pi^+\pi^-$ can be fully described by the Λ scattering angle in the center-of-mass (CM) system of the e^+e^- reaction, θ_Λ , and the p (\bar{p}) direction in the rest frame of its parent particle, $\hat{\mathbf{n}}_1$ ($\hat{\mathbf{n}}_2$). Here γ^*/Ψ represents that the process $e^+e^- \rightarrow \Lambda\bar{\Lambda}$ is produced by pure EM process or ψ resonance. The components of these vectors are expressed using a coordinate system $(x_\Lambda, y_\Lambda, z_\Lambda)$ with the orientation shown in Fig. 2. A right-handed system for each hyperon decay is defined here, with the z axis along the Λ momentum $\mathbf{p}_\Lambda = -\mathbf{p}_{\bar{\Lambda}} = \mathbf{p}$ in the CM system. The y axis is taken as the normal to the scattering plane, $\mathbf{k}_{e^-} \times \mathbf{p}_\Lambda$, where $\mathbf{k}_{e^-} = -\mathbf{k}_{e^+} = \mathbf{k}$ is the electron beam momentum in the CM system. For the determination of the modulus of the EM-*psionic* form factors R^Ψ [27] and relative phase $\Delta\Phi^\Psi$, the angular distribution parameter η (but not its absolute normalization) is of interest. In Ref. [26], the joint decay angular distribution of the process $e^+e^- \rightarrow \gamma^*/\Psi \rightarrow \Lambda\bar{\Lambda} \rightarrow p\bar{p}\pi^+\pi^-$ is expressed in terms of the phase $\Delta\Phi^\Psi$ and the angular distribution

$$\begin{aligned}
\mathcal{W}(\boldsymbol{\xi}; \boldsymbol{\Omega}) = & 1 + \eta \cos^2 \theta_\Lambda \\
& + \alpha_\Lambda \alpha_{\bar{\Lambda}} [\sin^2 \theta_\Lambda (n_{1,x} n_{2,x} - \eta n_{1,y} n_{2,y}) \\
& + (\cos^2 \theta_\Lambda + \eta) n_{1,z} n_{2,z}] \\
& + \alpha_\Lambda \alpha_{\bar{\Lambda}} [\sqrt{1 - \eta^2} \cos(\Delta\Phi^\Psi) \sin \theta_\Lambda \cos \theta_\Lambda (n_{1,x} n_{2,z} \\
& + n_{1,z} n_{2,x})] \\
& + \sqrt{1 - \eta^2} \sin(\Delta\Phi^\Psi) \sin \theta_\Lambda \cos \theta_\Lambda (\alpha_\Lambda n_{1,y} + \alpha_{\bar{\Lambda}} n_{2,y}),
\end{aligned} \tag{4.1}$$

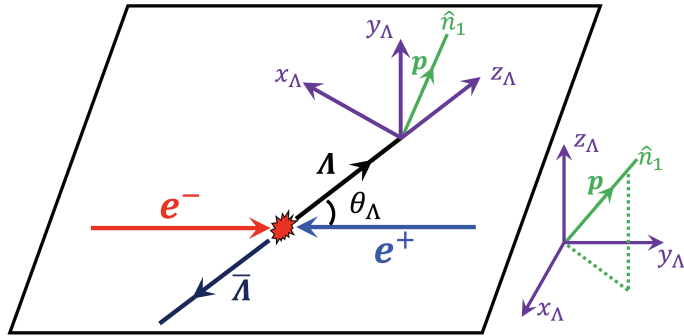


Figure 2. Definition of the coordinate system used to describe the $e^+e^- \rightarrow \gamma^*/\Psi \rightarrow \Lambda\bar{\Lambda} \rightarrow p\bar{p}\pi^+\pi^-$ reaction. The Λ particle is emitted along the z_Λ axis direction, and the $\bar{\Lambda}$ in the opposite direction. The y_Λ axis is perpendicular to the plane of Λ and e^- , and the x_Λ axis is defined by a right-handed coordinate system. The Λ decay product, the proton, is measured in this coordinate system.

where $\mathbf{\Omega} = (\eta, \Delta\Phi, \alpha_\Lambda, \alpha_{\bar{\Lambda}})$ represent the production and decay parameters, the kinematic variables $\boldsymbol{\xi} = (\theta_\Lambda, \hat{\mathbf{n}}_1, \hat{\mathbf{n}}_2)$ describe the production and subsequent decay, and $\alpha_{\Lambda(\bar{\Lambda})}$ denotes the decay asymmetry of the $\Lambda(\bar{\Lambda}) \rightarrow p\pi^-(\bar{p}\pi^+)$ decay process. The scattering angle distribution parameter η , is related to the ratio R^Ψ by

$$R^\Psi = \sqrt{\frac{\tau(1-\eta)}{1+\eta}}, \quad (4.2)$$

where $\tau = \frac{s}{4m_\Lambda^2}$, m_Λ is the known Λ mass [55], and s is the square of the CM energy. If the initial state is unpolarized, and the production process is either strong or electromagnetic and hence parity-conserving, then a non-zero polarization is only possible in the transverse direction y . The polarization is given by

$$P_y = \frac{\sqrt{1-\eta^2} \sin\theta_\Lambda \cos\theta_\Lambda}{1+\eta \cos^2\theta_\Lambda} \sin(\Delta\Phi^\Psi). \quad (4.3)$$

To determine the set of Λ spin polarization parameters $\mathbf{\Omega}$, an unbinned maximum likelihood fit is performed to extract the decay parameters, where the decay parameters $\alpha_{\Lambda/\bar{\Lambda}}$ are fixed to the value 0.754 obtained from the average in Ref. [36] assuming CP conservation. In the fit, the likelihood function \mathcal{L} is constructed from the probability function, $\mathcal{P}(\boldsymbol{\xi}_i)$, for an event i characterized by the measured angles $\boldsymbol{\xi}_i$

$$\mathcal{L} = \prod_{i=1}^N \mathcal{P}(\boldsymbol{\xi}_i, \mathbf{\Omega}) = \prod_{i=1}^N c\mathcal{W}(\boldsymbol{\xi}_i, \mathbf{\Omega})\epsilon(\boldsymbol{\xi}_i), \quad (4.4)$$

where N is the number of events in the signal region. The joint angular distribution $\mathcal{W}(\boldsymbol{\xi}_i, \mathbf{\Omega})$ is given in Eq. (4.1), and $\epsilon(\boldsymbol{\xi}_i)$ is the detection efficiency. As for the ISR effect at higher energy points 3.691 and 3.710 GeV, studies based on MC simulations are performed and the contribution from ISR process is negligible, where the input cross section

for $e^+e^- \rightarrow \Lambda\bar{\Lambda}$ for calculating the ISR effect is taken from Ref. [56]. The normalization factor $\mathcal{C} = \frac{1}{N_{\text{MC}}} \sum_{j=1}^{N_{\text{MC}}} \mathcal{W}(\boldsymbol{\xi}^j, \boldsymbol{\Omega})$ is given by the sum of the corresponding angular distribution function \mathcal{W} using the accepted MC events N_{MC} , and the difference between data and MC simulations is taken into account. The minimization of the function

$$\mathcal{S} = -\ln\mathcal{L}_{data} + \ln\mathcal{L}_{bg}, \quad (4.5)$$

is performed with the RooFit package [57]. Here, \mathcal{L}_{data} is the likelihood function of events selected in the signal region, and \mathcal{L}_{bg} is the likelihood function of background events determined in the sideband regions and continuum contribution, where continuum contribution is normalized by taking into account the luminosity and CM energy dependence of the cross section using the energy points at $\sqrt{s} = 3.581$ GeV, i.e.

$$N_{con.} = N_{3.581} \times \frac{\mathcal{L}_{Nom.}}{\mathcal{L}_{3.581}} \times \frac{s_{3.581}}{s_{Nom.}}, \quad (4.6)$$

where $N_{con.}$ is the normalized event for continuum process and $N_{3.581} = 12$, $\mathcal{L}_{3.581}$ and $s_{3.581}$ are the number of observed events, the luminosity and CM energy. The $\mathcal{L}_{Nom.}$, $s_{Nom.}$ are the luminosity and CM energy for each energy point and combined one in this work. Note that since the statistics for this analysis is limited, the background effect is taken into account in the part of systematic uncertainty later. Figure 3 shows distributions of the five moments [26]

$$\begin{aligned} F_1 &= \sum_{i=1}^{N_k} (\sin^2\theta_\Lambda n_{1,x}^i n_{2,x}^i + \cos^2\theta_\Lambda n_{1,z}^i n_{2,z}^i), \\ F_2 &= \sum_{i=1}^{N_k} \sin\theta_\Lambda \cos\theta_\Lambda (n_{1,x}^i n_{2,z}^i + n_{1,z}^i n_{2,x}^i), \\ F_3 &= \sum_{i=1}^{N_k} \sin\theta_\Lambda \cos\theta_\Lambda n_{1,y}^i, \\ F_4 &= \sum_{i=1}^{N_k} \sin\theta_\Lambda \cos\theta_\Lambda n_{2,y}^i, \\ F_5 &= \sum_{i=1}^{N_k} (n_{1,z}^i n_{2,z}^i - \sin^2\theta_\Lambda n_{1,y}^i n_{2,y}^i), \end{aligned} \quad (4.7)$$

with respect to $\cos\theta_\Lambda$, which are calculated for 10 intervals in $\cos\theta_\Lambda$. Here, N_k is the number of events in the k^{th} $\cos\theta_\Lambda$ interval, and i is the index from 1 to N_k . The numerical fit results, with asymmetric uncertainties, are summarized in Table 2 and Table 3, which are consistent with theoretical predictions [58]. The results presented in Table 2 are the combined values for merging all scan energy points for ψ resonance compared with the results from J/ψ and $\psi(3770)$, which could provide more insights into the underlying production mechanism of hyperon anti-hyperon pairs at different charmonium states and different energy points. Figure 4 shows the result of the hyperon transverse polarization P_y distribution, which is

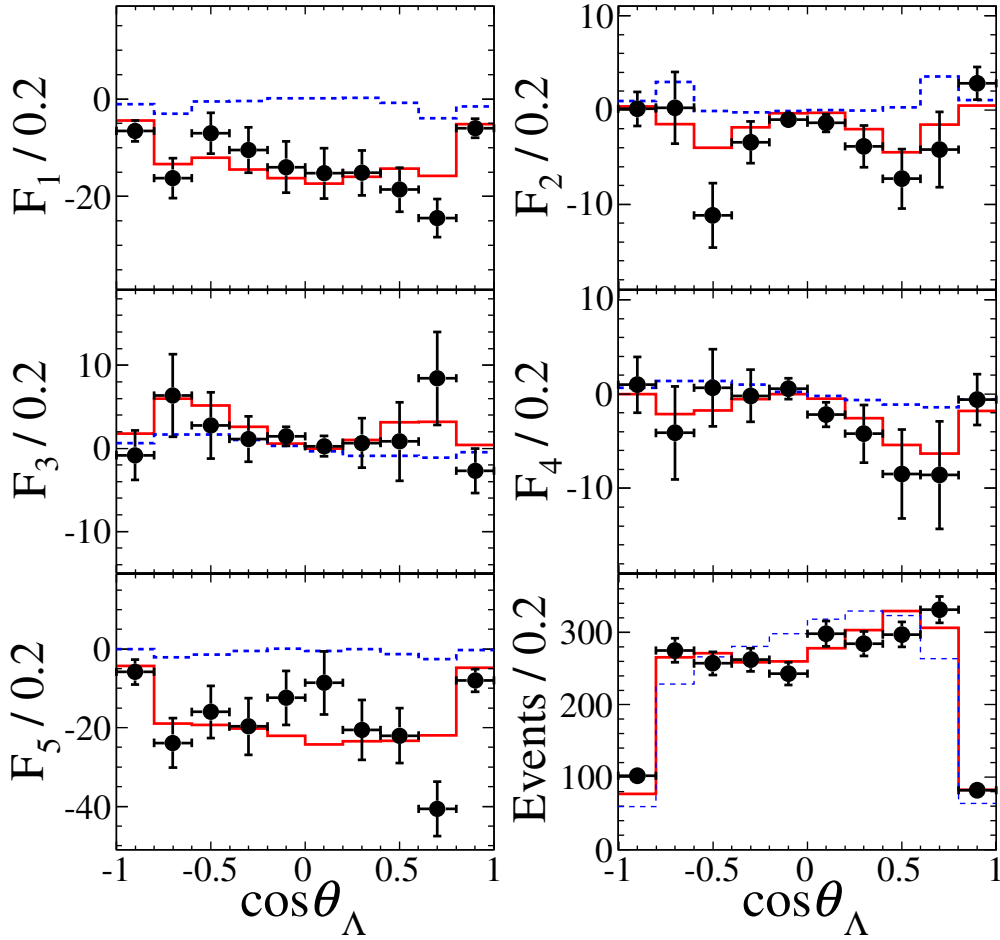


Figure 3. Distributions of F_k ($k = 1, 2, \dots, 5$) moments with respect to the $\cos\theta_\Lambda$ and the $\cos\theta_\Lambda$ distribution (bottom right). The dots with error bars are data from total energy points, and the red solid lines are the weighted PHSP MC corrected by the results of global fit. The blue dashed lines represent the distributions of the simulated events evenly distributed in phase space, without polarization.

consistent with the behavior of Eq. (4.3) as compared to the data. The moment given by

$$M(\cos\theta_\Lambda) = \frac{m}{N} \sum_{i=1}^{N_k} (n_{1,y}^i - n_{2,y}^i), \quad (4.8)$$

is related to the polarization, and calculated for $m = 10$ intervals in $\cos\theta_\Lambda$. Here, N represents the total number of events in the data sample. Assuming CP conservation, we have $\alpha_\Lambda = -\alpha_{\bar{\Lambda}}$, and the expected angular dependence is $M(\cos\theta_\Lambda)$, which is proportional to $\sqrt{1 - \eta^2} \alpha_\Lambda \sin\Delta\Phi^\Psi \cos\theta_\Lambda \sin\theta_\Lambda$ as shown in Fig. 4 according to Eq. (4.1).

The relative phase of the EM-*psionic* form factors is different from zero with a significance of 2.6σ including systematic uncertainty, and is estimated by comparing the likelihoods of the baseline fit and the one defined assuming no polarization. The effects of sys-

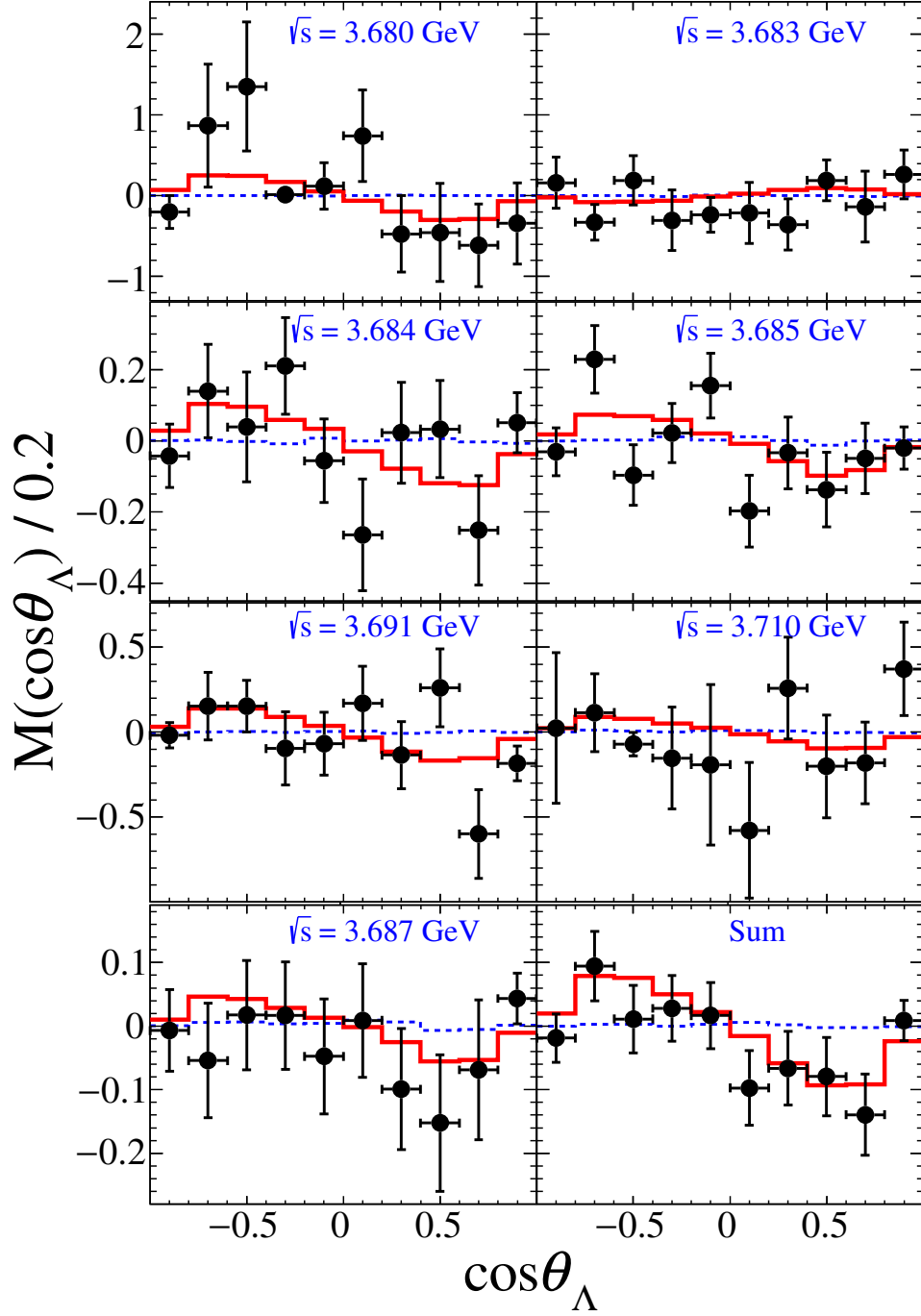


Figure 4. The moment $M(\cos\theta_\Lambda)$ as a function of $\cos\theta_\Lambda$ for the $e^+e^- \rightarrow \Lambda\bar{\Lambda}$ reaction around $\sqrt{s} = 3.686$ GeV. Points with error bars are data, the red solid lines are the weighted PHSP MC corrected by the results of global fit, and the blue dashed lines represent the distributions without polarization from simulated events, evenly distributed in the phase space.

tematic uncertainty are estimated conservatively by varying the decay parameters $\alpha_\Lambda(\alpha_{\bar{\Lambda}})$ by one standard deviation and by considering the employed requirements, respectively, and the combination with the smallest significance is adopted.

5 Systematic uncertainties

5.1 Λ reconstruction

The uncertainty due to the Λ reconstruction combined with the tracking and particle identification is determined from a control sample of $J/\psi \rightarrow \Lambda\bar{\Lambda}$ events with the same method as used in Ref. [27].

5.2 Mass window

The uncertainty due to the requirements on the $p\pi^-$ mass window is estimated with the smearing method as introduced in Ref. [38].

5.3 4C kinematic fit

The uncertainty due to 4C kinematic fit is estimated using the helix correction method mentioned in Ref. [59]. We repeat the fit procedure using the MC sample corrected by the track parameters, and take the difference between both results as the related systematic uncertainty.

5.4 Background

The systematic uncertainty due to the background is estimated in the fit of the parameter extraction with and without the contributions of sideband and continuum backgrounds. The difference is taken as the systematic uncertainty.

5.5 Fit method

To validate the reliability of the fit results, an input and output check based on 400 pseudoexperiments is performed with the helicity amplitude formula given in Ref. [26]. The polarization parameters measured in this analysis are used as input in the formula, and the number of events in each generated MC sample is nearly equal to the number in data sample. The differences between the input value and output value are taken as the systematic uncertainty by fitting method.

5.6 Decay parameter

The uncertainties from the decay parameters of $\Lambda \rightarrow p\pi^-$, $\alpha_{\Lambda/\bar{\Lambda}}$, are estimated by varying the baseline value, obtained from averaging the results in Ref. [36], by $\pm 1\sigma$. The largest difference in the result is taken as the systematic uncertainty.

5.7 Summary of systematic uncertainty

Assuming all sources are independent, the total systematic uncertainties on the measurement of the polarization parameters for the $e^+e^- \rightarrow \Lambda\bar{\Lambda} \rightarrow p\bar{p}\pi^+\pi^-$ process are determined by the square root of the quadratic sum of these sources as listed in Table 1.

Table 1. Summary of absolute value of the systematic uncertainty of polarization parameters.

Source	η	$\Delta\Phi^\Psi$ ($^\circ$)
Λ reconstruction	0.002	0.057
Mass window	0.012	0.286
4C kinematic fit	0.001	0.286
Sideband Background	0.009	1.375
Continuum Background	0.001	0.516
Fit method	0.001	0.115
Decay parameter	0.005	0.573
Total	0.016	1.633

6 Summary

In summary, we measure the Λ hyperon transverse polarization in the $e^+e^- \rightarrow \Lambda\bar{\Lambda}$ reaction at CM energies between 3.68 and 3.71 GeV, using a data sample corresponding to an integrated luminosity of 333 pb^{-1} collected with the BESIII detector at BEPCII. By combining the seven energy points, the relative phase and the modulus of the ratio of the EM-*psionic* form factors and the angular distribution parameter are determined, respectively. The relative phase is determined to be different from zero with a significance of 2.6σ including the systematic uncertainty. The comparison between our result and previous measurements in $e^+e^- \rightarrow \Lambda\bar{\Lambda}$ at 2.396 GeV [37] and $J/\psi \rightarrow \Lambda\bar{\Lambda}$ [36] is summarized in Table 2. The value from the phase obtained in $\psi(3686)$ resonance is roughly consistent with the measurement from $\psi(3770)$ decay and e^+e^- annihilation at $\sqrt{s} = 2.396$ GeV within the uncertainty of 1σ , but deviate from the measurement with J/ψ decay by 2.4σ . The η values are obviously different from the ones for J/ψ peak and $\sqrt{s} = 2.396$ GeV, but roughly consistent with the $\psi(3770)$ one. This implies the presence of different $e^+e^- \rightarrow \Lambda\bar{\Lambda}$ production mechanisms. More data samples at different energy points are needed for a detailed understanding for the underlying $\Lambda\bar{\Lambda}$ production mechanism and the structure of the Λ hyperon.

Table 2. The measured parameters from $\psi(3686)$ resonance for merging all scan energy points compared with previous measurements by combining the seven energy points. For each measurement, the first uncertainty is statistical and the second one is systematic.

Para.	η	$\Delta\Phi^\Psi$ ($^\circ$)	R^Ψ
This work (Sum)	$0.69^{+0.07}_{-0.07} \pm 0.02$	$23^{+8.8}_{-8.0} \pm 1.6$	$0.71^{+0.10}_{-0.10} \pm 0.03$
$\psi(3770) \rightarrow \Lambda\bar{\Lambda}$ [27]	$0.85^{+0.12}_{-0.20} \pm 0.02$	$71^{+66}_{-46} \pm 5$	$0.48^{+0.21}_{-0.35} \pm 0.04$
$J/\psi \rightarrow \Lambda\bar{\Lambda}$ [36]	$0.4748 \pm 0.0022 \pm 0.0031$	$43.09 \pm 0.24 \pm 0.38$	$0.8283 \pm 0.0024 \pm 0.0033$
$e^+e^- \rightarrow \Lambda\bar{\Lambda}$ ($\sqrt{s} = 2.396$ GeV) [37]	$0.12 \pm 0.14 \pm 0.02$	$37 \pm 12 \pm 6$	$0.96 \pm 0.14 \pm 0.02$

Acknowledgments

The BESIII collaboration thanks the staff of BEPCII and the IHEP computing center for their strong support. This work is supported in part by National Key R&D Program of

Table 3. The number of observed events N_{obs} (from the S region defined in Fig. 1) and measured parameters η , $\Delta\Phi$ and R^Ψ for each energy point. For each measurement, the first uncertainty is statistical and the second one is systematic.

\sqrt{s} (MeV)	N_{obs}	η	$\Delta\Phi(^{\circ})$	R^Ψ
3680	31^{+7}_{-6}	$0.12^{+0.46}_{-0.43} \pm 0.02$	$110.6^{+34.4}_{-37.8} \pm 1.6$	$1.46^{+0.68}_{-0.64} \pm 0.03$
3683	78^{+10}_{-9}	$0.95^{+0.18}_{-0.20} \pm 0.02$	$-108.9^{+181.6}_{-185.6} \pm 1.6$	$0.26^{+0.49}_{-0.54} \pm 0.05$
3684	385^{+21}_{-20}	$0.59^{+0.18}_{-0.18} \pm 0.02$	$28.0^{+24.1}_{-18.3} \pm 1.6$	$0.84^{+0.54}_{-0.23} \pm 0.02$
3685	831^{+30}_{-29}	$0.64^{+0.11}_{-0.12} \pm 0.02$	$20.1^{+12.6}_{-12.0} \pm 1.6$	$0.77^{+0.14}_{-0.15} \pm 0.03$
3687	876^{+31}_{-30}	$0.71^{+0.12}_{-0.13} \pm 0.02$	$12.0^{+14.9}_{-13.2} \pm 1.6$	$0.68^{+0.16}_{-0.18} \pm 0.03$
3691	176^{+14}_{-13}	$0.83^{+0.14}_{-0.23} \pm 0.02$	$112.9^{+44.1}_{-63.0} \pm 1.6$	$0.50^{+0.23}_{-0.37} \pm 0.03$
3710	53^{+8}_{-7}	$0.52^{+0.38}_{-0.39} \pm 0.02$	$0.0^{+64.7}_{-56.7} \pm 1.6$	$0.93^{+0.49}_{-0.50} \pm 0.03$

China under Contracts Nos. 2020YFA0406400, 2020YFA0406300; National Natural Science Foundation of China (NSFC) under Contracts Nos. 12075107, 12247101, 11635010, 11735014, 11835012, 11935015, 11935016, 11935018, 11961141012, 12022510, 12025502, 12035009, 12035013, 12061131003, 12192260, 12192261, 12192262, 12192263, 12192264, 12192265; the Chinese Academy of Sciences (CAS) Large-Scale Scientific Facility Program; Supported by the 111 Project under Grant No. B20063; the CAS Center for Excellence in Particle Physics (CCEPP); Joint Large-Scale Scientific Facility Funds of the NSFC and CAS under Contract No. U1832207; CAS Key Research Program of Frontier Sciences under Contracts Nos. QYZDJ-SSW-SLH003, QYZDJ-SSW-SLH040; 100 Talents Program of CAS; The Institute of Nuclear and Particle Physics (INPAC) and Shanghai Key Laboratory for Particle Physics and Cosmology; ERC under Contract No. 758462; European Union’s Horizon 2020 research and innovation programme under Marie Skłodowska-Curie grant agreement under Contract No. 894790; German Research Foundation DFG under Contracts Nos. 443159800, 455635585, Collaborative Research Center CRC 1044, FOR5327, GRK 2149; Istituto Nazionale di Fisica Nucleare, Italy; Ministry of Development of Turkey under Contract No. DPT2006K-120470; National Science and Technology fund; National Science Research and Innovation Fund (NSRF) via the Program Management Unit for Human Resources & Institutional Development, Research and Innovation under Contract No. B16F640076; Olle Engkvist Foundation under Contract No. 200-0605; Polish National Science Centre under Contract No. 2019/35/O/ST2/02907; STFC (United Kingdom); Suranaree University of Technology (SUT), Thailand Science Research and Innovation (TSRI), and National Science Research and Innovation Fund (NSRF) under Contract No. 160355; The Royal Society, UK under Contracts Nos. DH140054, DH160214; The Swedish Research Council; U. S. Department of Energy under Contract No. DE-FG02-05ER41374.

References

- [1] S. J. Brodsky and G. R. Farrar, *Scaling laws for large-momentum-transfer processes*, *Phys. Rev. D* **11**, 1309 (1975) [INSPIRE].
- [2] L. S. Geng, J. Martin Camalich, L. Alvarez-Ruso and M. J. Vicente Vacas, *Leading $SU(3)$ -Breaking Corrections to the Baryon Magnetic Moments in Chiral Perturbation Theory*, *Phys. Rev. Lett.* **101**, 222002 (2008) [arXiv:0805.1419] [INSPIRE].

- [3] J. R. Green, J. W. Negele, A. V. Pochinsky, S. N. Syritsyn, M. Engelhardt and S. Krieg, *Nucleon electromagnetic form factors from lattice QCD using a nearly physical pion mass*, *Phys. Rev. D* **90**, 074507 (2014) [arXiv:1404.4029] [INSPIRE].
- [4] X. F. Wang and G. S. Huang, *Electromagnetic form factor of doubly-strange hyperon*, *Symmetry* **14**, 65 (2022) [INSPIRE].
- [5] X.F. Wang, *Hyperon pair production at BESIII*, *Rev. Mex. Fis. Suppl.* **3**, 0308074 (2022) [INSPIRE].
- [6] H. Liu, J. Zhang and X. Wang, *CP asymmetry in the Ξ hyperon sector*, *Symmetry* **15**, 214 (2023) [INSPIRE].
- [7] N. Cabibbo and R. Gatto, *Electron-positron colliding beam experiments*, *Phys. Rev.* **124**, 1577 (1961) [INSPIRE].
- [8] M. A. Belushkin, H. -W. Hammer and Ulf-G. Meißner, *Dispersion analysis of the nucleon form factors including meson continua*, *Phys. Rev. C* **75**, 035202 (2007) [arXiv:hep-ph/0608337] [INSPIRE].
- [9] B. Yan, C. Chen and J. J. Xie, *Σ and Ξ electromagnetic form factors in the extended vector meson dominance model*, *Phys. Rev. D* **107**, 076008 (2023) [arXiv:2301.00976] [INSPIRE].
- [10] G. S. Huang, R. B. Ferroli and BESIII Collaboration, *Probing the internal structure of baryons*, *Natl. Sci. Rev.* **8**(11), nwab187 (2021) [INSPIRE].
- [11] R. Q. Qian, Q. Huang and X. Liu, *Predicted $\Lambda\bar{\Lambda}$ and $\Xi^-\bar{\Xi}^+$ decay modes of the charmoniumlike $Y(4230)$* , *Phys. Lett. B* **833**, 137292 (2022) [arXiv:2111.13821] [INSPIRE].
- [12] BABAR Collaboration, *Measurement of the inclusive jet cross section using the k_T algorithm in $p\bar{p}$ collisions at $\sqrt{s} = 1.96$ TeV with the CDF II detector*, *Phys. Rev. D* **76**, 092006 (2007) [arXiv:hep-ex/0701051] [INSPIRE].
- [13] S. Dobbs, A. Tomaradze, T. Xiao, K. K. Seth and G. Bonvicini, *First measurements of timelike form factors of the hyperons, $\Lambda^0, \Sigma^0, \Sigma^+, \Xi^0, \Xi^-,$ and Ω^- , and evidence of diquark correlations*, *Phys. Lett. B* **739**, 90 (2014) [arXiv:1410.8356] [INSPIRE].
- [14] S. Dobbs, K. K. Seth, A. Tomaradze, T. Xiao and G. Bonvicini, *Hyperon form factors and diquark correlations*, *Phys. Rev. D* **96**, 092004 (2017) [arXiv:1708.09377] [INSPIRE].
- [15] R. Jaffe, *Exotica*, *Phys. Rep.* **409**, 1–45 (2005) [arXiv:hep-ph/0409065] [INSPIRE].
- [16] R. Jaffe, F. Wilczek, *Diquarks and exotic spectroscopy*, *Phys. Rev. Lett.* **91**, 232003 (2003) [arXiv:hep-ph/0307341] [INSPIRE].
- [17] BESIII Collaboration, *Observation of a cross-section enhancement near mass threshold in $e^+e^- \rightarrow \Lambda\bar{\Lambda}$* , *Phys. Rev. D* **97**, 032013 (2018) [arXiv:1709.10236] [INSPIRE].
- [18] BESIII Collaboration, *Measurements of Σ^+ and Σ^- time-like electromagnetic form factors for center-of-mass energies from 2.3864 to 3.0200 GeV*, *Phys. Lett. B* **814**, 136110 (2021) [arXiv:2009.01404] [INSPIRE].
- [19] BESIII Collaboration, *Measurement of cross section for $e^+e^- \rightarrow \Xi^-\bar{\Xi}^+$ near threshold at BESIII*, *Phys. Rev. D* **103**, 012005 (2021) [arXiv:2010.08320] [INSPIRE].
- [20] BESIII Collaboration, *Measurement of cross section for $e^+e^- \rightarrow \Xi^0\bar{\Xi}^0$ near threshold*, *Phys. Lett. B* **820**, 136557 (2021) [arXiv:2105.14657] [INSPIRE].

- [21] BESIII Collaboration, *Measurement of the $e^+e^- \rightarrow \Sigma^0\bar{\Sigma}^0$ cross sections at center-of-mass energies from 2.3864 to 3.0200 GeV*, *Phys. Lett. B* **831**, 137187 (2022) [arxiv:2110.04510] [INSPIRE].
- [22] BESIII Collaboration, *Study of $e^+e^- \rightarrow \Omega^-\bar{\Omega}^+$ at center-of-mass energies from 3.49 to 3.67 GeV*, *Phys. Rev. D* **107**, 052003 (2023) [arxiv:2212.03693] [INSPIRE].
- [23] BESIII Collaboration, *Measurement of the cross section for $e^+e^- \rightarrow \Xi^-\bar{\Xi}^+$ and observation of an excited Ξ baryon*, *Phys. Rev. Lett.* **124**, 032002 (2020) [arxiv:1910.04921] [INSPIRE].
- [24] BESIII Collaboration, *Measurement of the cross section of $e^+e^- \rightarrow \Xi^-\bar{\Xi}^+$ at center-of-mass energies between 3.510 and 4.843 GeV*, [arXiv:2302.09767] [INSPIRE].
- [25] BESIII Collaboration, *Measurement of the cross section for $e^+e^- \rightarrow \Lambda\bar{\Lambda}$ and evidence of the decay $\psi(3770) \rightarrow \Lambda\bar{\Lambda}$* , *Phys. Rev. D* **104**, L091104 (2021) [arxiv:2108.02410] [INSPIRE].
- [26] G. Fäldt and A. Kupsc, *Hadronic structure functions in the $e^+e^- \rightarrow \bar{\Lambda}\Lambda$ reaction*, *Phys. Lett. B* **772**, 16 (2017) [arxiv:1702.07288] [INSPIRE].
- [27] BESIII Collaboration, *Measurement of Λ baryon polarization in $e^+e^- \rightarrow \Lambda\bar{\Lambda}$ at $\sqrt{s} = 3.773$ GeV*, *Phys. Rev. D* **105**, L011101 (2022) [arxiv:2111.11742] [INSPIRE].
- [28] BESIII Collaboration, *Measurements of baryon pair decays of χ_{cJ} mesons*, *Phys. Rev. D* **87**, 032007 (2013) [arxiv:1211.2283] [INSPIRE].
- [29] BESIII Collaboration, *Study of ψ decays to the $\Xi^-\bar{\Xi}^+$ and $\Sigma(1385)^+\bar{\Sigma}(1385)^{\pm}$ final states*, *Phys. Rev. D* **93**, 072003 (2016) [arxiv:1602.06754] [INSPIRE].
- [30] BESIII Collaboration, *Study of J/ψ and $\psi(3686) \rightarrow \Sigma(1385)^0\bar{\Sigma}(1385)^0$ and $\Xi^0\bar{\Xi}^0$* , *Phys. Lett. B* **770**, 217 (2017) [arxiv:1612.08664] [INSPIRE].
- [31] BESIII Collaboration, *Observation of $\psi(3686) \rightarrow \Xi(1530)^-\bar{\Xi}(1530)^+$ and $\Xi(1530)^-\bar{\Xi}^+$* , *Phys. Rev. D* **100**, 051101 (2019) [arxiv:1907.13041] [INSPIRE].
- [32] X. F. Wang, B. Li, Y. N. Gao and X. C. Lou, *Helicity amplitude analysis of J/ψ and $\psi(3686) \rightarrow \Xi(1530)\bar{\Xi}(1530)$* , *Nucl. Phys. B* **941**, 861 (2019) [arxiv:1811.11352] [INSPIRE].
- [33] X. F. Wang, *Study of baryon pair production at BESIII*, *PoS CHARM2020*, 026 (2021) [INSPIRE].
- [34] BESIII Collaboration, *Study of the processes $\chi_{cJ} \rightarrow \Xi^-\bar{\Xi}^+$ and $\Xi^0\bar{\Xi}^0$* , *JHEP* **06**, 74 (2022) [arxiv:2202.08058] [INSPIRE].
- [35] BESIII Collaboration, *Polarization and entanglement in baryon-antibaryon pair production in electron-positron annihilation*, *Nature Phys.* **15**, 631 (2019) [arxiv:1808.08917] [INSPIRE].
- [36] BESIII Collaboration, *Precise measurements of decay parameters and CP asymmetry with entangled $\Lambda-\bar{\Lambda}$ pairs*, *Phys. Rev. Lett.* **129**, 131801 (2022) [arxiv:2204.11058] [INSPIRE].
- [37] BESIII Collaboration, *Complete Measurement of the Λ Electromagnetic Form Factors*, *Phys. Rev. Lett.* **123**, 122003 (2019) [arxiv:1903.09421] [INSPIRE].
- [38] BESIII Collaboration, *Σ^+ and $\bar{\Sigma}^-$ polarization in the J/ψ and $\psi(3686)$ decays*, *Phys. Rev. Lett.* **125**, 052004 (2020) [arxiv:2004.07701] [INSPIRE].
- [39] BESIII Collaboration, *Probing CP symmetry and weak phases with entangled double-strange baryons*, *Nature* **606**, 64 (2022) [arxiv:2105.11155] [INSPIRE].
- [40] BESIII Collaboration, *Observation of Ξ^- hyperon transverse polarization in $\psi(3686) \rightarrow \Xi^-\bar{\Xi}^+$* , *Phys. Rev. D* **106**, L091101 (2022) [arxiv:2206.10900] [INSPIRE].

- [41] BESIII Collaboration, *First simultaneous measurement of Ξ^0 and $\bar{\Xi}^0$ asymmetry parameters in $\psi(3686)$ decay*, [[arXiv:2302.09767](#)] [[INSPIRE](#)].
- [42] BESIII Collaboration, *Design and construction of the BESIII detector*, *Nucl. Instrum. Meth. A* **614**, 345 (2010) [[arxiv:0911.4960](#)] [[INSPIRE](#)].
- [43] C. H. Yu *et al.*, *BEPCII Performance and Beam Dynamics Studies on Luminosity, Proceedings of IPAC2016, Busan, Korea, (2016)* [[INSPIRE](#)].
- [44] BESIII Collaboration, *Future Physics Programme of BESIII*, *Chin. Phys. C* **44** (2020) 040001 [[arXiv:1912.05983](#)] [[INSPIRE](#)].
- [45] X. Li *et al.*, *Study of MRPC technology for BESIII endcap-TOF upgrade*, *Radiat. Detect. Technol. Methods* **1** 13 (2017).
- [46] Y. X. Guo *et al.*, *The study of time calibration for upgraded end cap TOF of BESIII*, *Radiat. Detect. Technol. Methods* **1** 15 (2017).
- [47] P. Cao *et al.*, *Design and construction of the new BESIII endcap Time-of-Flight system with MRPC Technology*, *Nucl. Instrum. Meth. A* **953** (2020) 163053 [[INSPIRE](#)].
- [48] GEANT4 Collaboration, *GEANT4—a simulation toolkit*, *Nucl. Instrum. Meth. A* **506** (2003) 250 [[INSPIRE](#)].
- [49] K. X. Huang, Z. J. Li, Z. Qian, J. Zhu, H. Y. Li, Y. M. Zhang, S. S. Sun and Z. Y. You, *Method for detector description transformation to Unity and application in BESIII*, *Nucl. Sci. Tech.* **33** (2022) 142 [[arXiv:2206.10117](#)] [[INSPIRE](#)].
- [50] S. Jadach, B. F. L. Ward and Z. Was, *Coherent exclusive exponentiation for precision Monte Carlo calculations*, *Phys. Rev. D* **63** (2001) 113009 [[arXiv:hep-ph/0006359](#)] [[INSPIRE](#)].
- [51] D. J. Lange, *The EvtGen particle decay simulation package*, *Nucl. Instrum. Meth. A* **462** (2001) 152-155 [[INSPIRE](#)].
- [52] R. G. Ping, *Event generators at BESIII*, *Chin. Phys. C* **32** (2008) 599 [[INSPIRE](#)].
- [53] BESIII Collaboration, *Determination of the number of $\psi(3686)$ events at BESIII* *Chin. Phys. C* **42** 023001 (2018) [[arXiv:1709.03653](#)] [[INSPIRE](#)].
- [54] M. Xu *et al.*, *Decay vertex reconstruction and 3-dimensional lifetime determination at BESIII*, *Chin. Phys. C* **33**, 428 (2009) [[INSPIRE](#)].
- [55] Particle Data Group, *Review of Particle Physics*, *Prog. Theor. Exp. Phys.* **2022**, 083C01 (2022).
- [56] KEDR Collaboration, *Final analysis of KEDR data on J/ψ and $\psi(2S)$ masses*, *Phys. Lett. B* **749** 50 (2015) [[INSPIRE](#)].
- [57] W. Verkerke and D. P. Kirkby, *The RooFit toolkit for data modeling*, *eConf* **C0303241**, MOLT007 (2003) [[arXiv:physics/0306116](#)] [[INSPIRE](#)].
- [58] A. Mangoni, S. Pacetti and E. Tomasi-Gustafsson, *First exploration of the physical Riemann surfaces of the ratio G_E^Λ/G_M^Λ* , *Phys. Rev. D* **104** 116016 (2021) [[arXiv:2109.03759](#)] [[INSPIRE](#)].
- [59] BESIII Collaboration, *Search for hadronic transition $\chi_{cJ} \rightarrow \eta_c \pi^+ \pi^-$ and observation of $\chi_{cJ} \rightarrow K \bar{K} \pi \pi$* , *Phys. Rev. D* **87** 012002 (2013) [[arXiv:1208.4805](#)] [[INSPIRE](#)].